

# Modeling the Impact of Social Distancing on the COVID-19 Pandemic in a Low Transmission Setting

Junxiao Xue<sup>ID</sup>, Member, IEEE, Mingchuang Zhang<sup>ID</sup>, and Mingliang Xu<sup>ID</sup>, Member, IEEE

**Abstract**—According to the World Health Organization and the CDC, social distancing is currently one of the most effective ways to slow the transmission of COVID-19. However, most existing epidemic models do not consider the impact of social distancing on the COVID-19 pandemic. In this article, we propose a new method to deterministic modeling of the effects of social distancing on the COVID-19 pandemic in a low transmission setting. Our model dynamic is expressed by a single predictive variable that satisfies an integro-differential equation. Once the dynamic variable is calculated, the process of agents from the normal state, infection state to rehabilitation state, or death state can be explored. Besides, an important parameter is added to the model to measure the impact of social distancing on epidemic transmission. We performed qualitative and quantitative experiments on various scenarios, and the results showed that 2 m is a safe social distancing on the COVID-19 pandemic in a low transmission setting.

**Index Terms**—COVID-19, modeling, simulation, social distance.

## I. INTRODUCTION

THE study of emerging infectious diseases is a hot topic in infection biology. At the same time, it is an ancient topic. Infectious diseases can be traced back as far as ten thousand years ago to the Neolithic period [1], [2]. Global preparedness in response to a new infectious disease pandemic has improved. For example, after SARS in 2003, China thoroughly reformed public health surveillance and control methods, carried out major legislative reforms, and established the world's largest online infectious disease reporting system [3], [4]. However, the COVID-19 pandemic still exposes many problems, and pandemic preparedness remains a political and scientific challenge to the world [5].

Manuscript received December 29, 2020; revised September 23, 2021 and November 5, 2021; accepted November 15, 2021. This work was supported in part by the National Natural Science Foundation of China under Grant 62036010 and Grant 61972362 and in part by the Young Backbone Teachers in Henan Province under Grant 22020GGJS014. (Corresponding author: Mingchuang Zhang.)

Junxiao Xue is with the School of Cyberspace Security, Zhengzhou University, Zhengzhou 450002, China, and also with the State Key Laboratory of Wheat and Maize Crop Science, Henan Agricultural University, Zhengzhou 450002, China (e-mail: xuejx@zzu.edu.cn).

Mingchuang Zhang is with the School of Cyberspace Security, Zhengzhou University, Zhengzhou 450002, China (e-mail: zhangcm@gs.zzu.edu.cn).

Mingliang Xu is with the School of Information Engineering, Zhengzhou University, Zhengzhou 450001, China (e-mail: iexumingliang@zzu.edu.cn).

This article has supplementary downloadable material available at <https://doi.org/10.1109/TCSS.2021.3129309>, provided by the authors.

Digital Object Identifier 10.1109/TCSS.2021.3129309

Due to the lack of sanitation facilities, large-scale gatherings are likely to lead to the emergence of infectious diseases, and rapidly population movements may spread diseases throughout the world. Organizing a large-scale gathering in the context of the COVID-19 epidemic is a huge challenge. Many large-scale gatherings planned during the epidemic have also been canceled, such as the 2020 Tokyo Olympic Games, religious festivals, and concerts [3].

At present, there are many ways to alleviate COVID-19. Peak *et al.* [6] proposed a method for nucleic acid detection of close contacts and isolation control of those who tested positive. However, with the expansion of the epidemic, this approach poses a huge challenge to quarantine resources [6]. Some relatively underfunded countries and regions do not have the capacity to implement this approach. They need simpler, effective, and low-cost ways to cope with the epidemic [7].

Chu *et al.* [8] did a systematic review and analysis of the optimal distance for person-to-person virus transmission and evaluated the transmission of the virus by masks and glasses. Block *et al.* [9] evaluated the effectiveness of three distance strategies using a social network approach in order for people to move normally in a postepidemic controlled world. Nevertheless, we found that existing methods are not well considering the influence of social distance on the spread of the epidemic. Our primary aim is to set up a social distance-based COVID-19 epidemic transmission model in this article, which can simulate and analyze the transmission process of the COVID-19 epidemic and obtain the minimum social distance for interrupting the spread of the virus among people. Our major contributions are listed as follows.

- 1) We modified the traditional SIR model to the NIRD model and proposed a COVID-19 epidemic transmission model based on social distance.
- 2) Our approach differs from most purely mathematical models in that we incorporate the model directly in the agents and build the model modularly. The model has the advantages of high flexibility, reduced coupling of other modules to the whole, and easy debugging and upgrading of module functionality.
- 3) We performed sensitivity analysis on the model to derive a minimum social distance that managers can apply in real-world scenarios to suppress the transmission of COVID-19.

The remaining section of this article proceeds as follows. Section II introduces the related work of the model method. Section III is concerned with the methodology used for

this study. Section IV presents the research findings, focusing on the three key experiments: sensitivity analysis, simulation and comparison, and queue optimization. The last section summarizes the main contributions and shortcomings of this article and points out the future research directions.

## II. RELATED WORK

### A. SIR Model

The SIR model is a classic model in the infectious disease model. The model divides the population into three types: Type *S*(Susceptible), who is not infected, lack immunity, and are vulnerable to contact with infected people. Type *I*(Infective), who is already infected, it can be transmitted to the *S* group of people. Type *R*(Removal), is a person who is isolated or has immunity due to illness.

SIR is widely used in infectious disease research. Andrews and Basu [10] adopted the SIR model to simulate the transmission mechanism of cholera. It can also be applied to research on network information transmission. Chen *et al.* [12] detected multiple information sources in networks by the SIR model. Furthermore, many researchers will improve the SIR model according to the actual situation to achieve the research purpose [13]. For example, Chen *et al.* [14] modified the SIR model to propose the SVIQR model and used it to study those diseases that cannot lead to permanent immunity to infection.

### B. Agent-Based Simulation Modeling

Modeling and simulation are the most effective and economical methods for research work. Kou *et al.* [15] proposed a multiagent-based modeling and simulation technique that simulates the relationship between individual behavior and the overall performance of HST components. Besides, the technique can help to verify the design with the advantages of more intelligence, flexibility, and time saving.

Most of the existing epidemic simulation theories and experimental data are obtained from the Internet. It is difficult to reflect the real situation of the epidemic truly. Based on ethical considerations, it is impossible to conduct experiments in epidemic situations with real people. Therefore, it is of great display significance to deduce epidemic situations through virtual simulation based on agents [13]. For instance, Nakamura *et al.* [16] proposed two methods to implement spin symmetry, improve the performance of agent-based epidemic models, and simplify the process of disease transmission analysis in agent-based epidemic models.

Agents are characterized by perception, adaptability, autonomy, and collaboration. The proxy objects are equipped with adaptive evolution ability in the simulation and deduction of the model. An agent-based model is a set of interactive objects reflecting various relationships in the real world. In the COVID-19 epidemic model presented here, the agent is the population.

### C. Social Distancing

Social isolation has become one of the main mitigation strategies in many countries, forcing people to stay at home

and avoid close contact with others as much as possible to reduce the spread and intensity of the epidemic [17]. While the scientific basis for these interventions is strong, the isolation policies may bring about civil liberties restrictions, income reduction, and even the risk of unemployment. Therefore, they should only be carried out when necessary to protect public health [18], [19].

Social isolation requires the distance between people as far as possible, while social distance is as close as possible under the premise of security. Social distance is the preferred option to control the epidemic in some industries that resume work early, such as airlines, passenger transport, hospitals, and factories, to mitigate the negative impact of social isolation. Salari *et al.* [20] proposed a mixed integer programming model that uses two medium types of social distances to assign passengers as on the plane. Chandra *et al.* [21] compared the transmission of COVID-19 in India at different social distance rates, and the model was predicted for early COVID-19 transmission in India.

In this article, the key factor of social distance is added to the model to control the transmission of the epidemic by adjusting the value of social distance to obtain the minimum social distance.

## III. METHODOLOGY

This article proposes that the social distance based COVID-19 epidemic transmission model includes three important parts: scene module, agent module, and COVID-19 epidemic transmission module. As shown in Fig. 1.

The scene modeling module defines the agent's appearance, state, capacity, and building models, which are the active components and containers of the entire model. The agent modeling module modifies the SIR model. It adds the social distance factor, which is responsible for defining the agent's parameters and the change rate of people in various states. And the COVID-19 epidemic transmission model module defines the infection and cure mechanism of the model. In this section, we will introduce the implementation and functions of each module in detail.

### A. Scene Module

Scene modeling models the real scene, and intuitive observation models have realism and strong interaction characteristics, which can better simulate the scene when the epidemic is spreading. Each scene has two modules (agents and buildings).

1) *Definition of Agent Appearance:* The agent's state is defined as  $M(N_c, I_c, R_c, D_c)$ .  $N$  represents the normal state,  $I$  represents the infected state,  $R$  represents the recovery state, and  $D$  represents the death state.  $c$  represents the color of the agent in the current state.

The location and size of an agent are defined as  $M[(x_1, x_2), (y_1, y_2), (z_1, z_2)]$ .  $x_1, y_1, z_1$ , respectively, represent the agent's position in  $O - xyz$  (space rectangular coordinate system).  $x_2$  represents the size of the agent radius,  $z_2$  represents the height of an agent. The  $s$  (area) and  $v$  (volume)

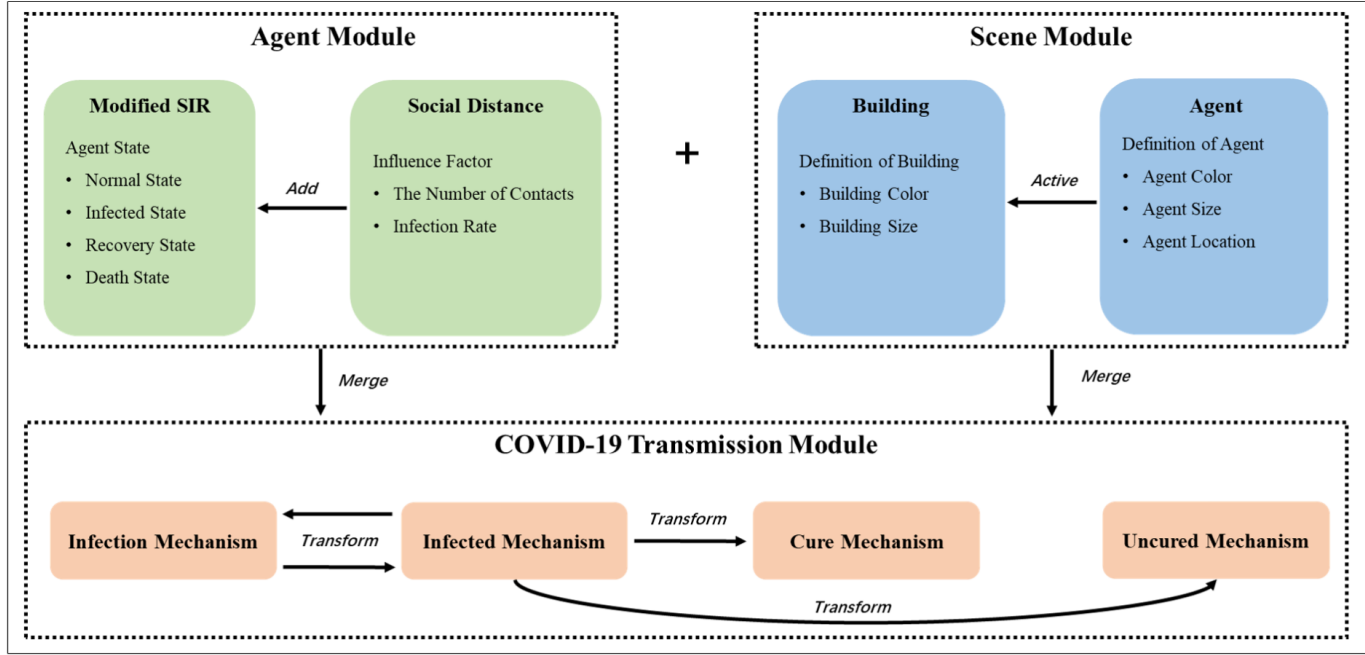


Fig. 1. Model overview: A social distance based COVID-19 epidemic transmission model.

occupied by a single agent in the scene are formulated as

$$\begin{cases} s = \pi \cdot (x_2)^2 \\ v = s \cdot z_2. \end{cases} \quad (1)$$

2) *Definition of Building:* The location and size of the building are defined as  $B\{X(a, b), Y(c, d), Z(e, f)\}$ .  $X_a, Y_c, Z_e$  represents the location of the building in  $O - xyz$ .  $X_b, Y_d, Z_f$  represents the length, width, and height of a building.

From the above definition, it can be concluded, the area and volume of the building are formulated as

$$\begin{cases} \text{area} = X_b \cdot Y_d \\ \text{volume} = X_b \cdot Y_d \cdot Z_f. \end{cases} \quad (2)$$

The maximum number of count (number of agents) that can be accommodated in a building is

$$\text{count} = [\min] \left\{ \frac{\text{area}}{\frac{s}{v}} \right\}. \quad (3)$$

After adding  $S_d$  (social distance), the number of agents that can be accommodated in the building will change to

$$\text{count} = [\min] \left\{ \frac{\text{area}}{\frac{s + S_d}{v}} \right\}. \quad (4)$$

The value of count is the maximum value in (3) and (4).  $[\min]$  indicates that count should be an integer.

Besides, the appearance of a building is defined as  $A(\text{color}, \text{wide}, \text{type})$ .  $A(\text{color})$  represents the color of the building's appearance.  $A(\text{wide})$  represents the thickness of the wall.  $A(\text{type})$  represents whether the building is passable, the type value of 0 means non pass, and the type value of 1 means pass.

## B. Agent Module

In the SIR model, the type  $R(\text{Removal})$  is a person who is isolated or has immune due to illness. However, in the COVID-19, those infected will die because they are not cured. We need to take those who die into account in the model to better modeling the agent. Therefore, this article divides the  $R$  population into  $R$  and  $D$ .  $R$  is a rehabilitee, the population in this state is immune and no longer participates in the spread of the epidemic.  $D$  is dead, the population in this state will be removed from the model.

In this model, the number of the four states of an agent is denoted as  $N(t), I(t), R(t), D(t)$ . They represent the number of people in the four states at time  $t$ . Assumptions the total population is  $P(t)$ , then

$$P(t) = N(t) + I(t) + R(t) + D(t). \quad (5)$$

The rate of change of the number of agents in the four states

$$\begin{cases} N' = N(t+1) - N(t) \\ I' = I(t+1) - I(t) \\ R' = R(t+1) - R(t) \\ D' = D(t+1) - D(t). \end{cases} \quad (6)$$

The COVID-19 transmission model based on social distance has three assumptions as follows.

- 1) The population flow factor is not considered. Namely, the crowd in the scene does not communicate with the outside world. The population in the scene always maintains a constant. We can define  $P(t) \equiv K$ .
- 2) The contact between an infected person and a normal person must have a certain infectious power. Assuming a unit time at time  $t$ , the number of normal states that an infected person can infect is proportional to the total

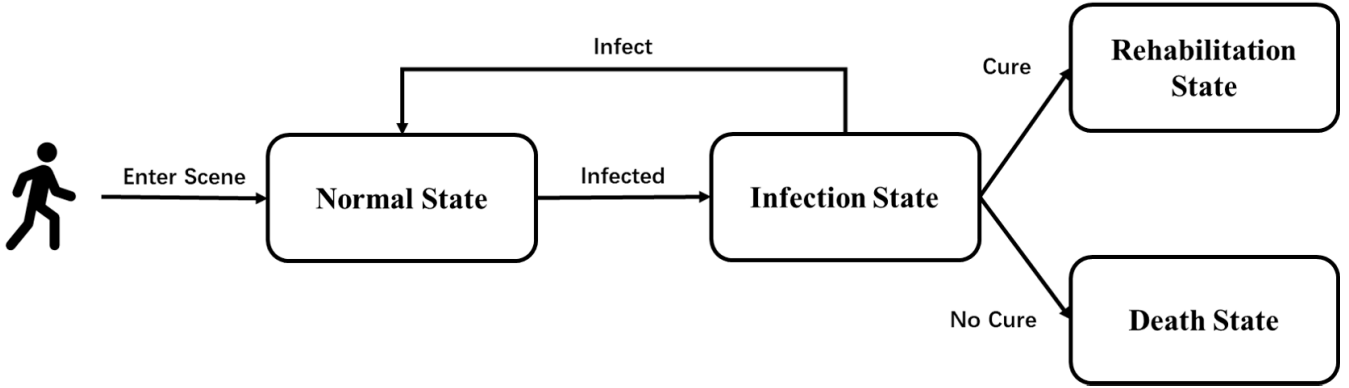


Fig. 2. Model transformation mechanism.

number of normal states in the environment  $N(t)$ ; The proportionality coefficient is  $\beta$ . It can be deduced that the number of people infected by all infected persons in a unit time is  $\beta \cdot N(t) \cdot I(t)$ .

- 3) At time  $t$ , the number of people cured and dead from infected persons per unit time is proportional to the number of infected persons, the proportional coefficient is  $\gamma$ , and the number of persons removed per unit time is  $\gamma \cdot I(t)$ .

Formulate it based on three assumptions

$$\begin{cases} N(t) + I(t+1) \xrightarrow{\beta} I(t) + I(t+1) \\ I(t) \xrightarrow{\gamma} R(t) + D(t). \end{cases} \quad (7)$$

From the above assumptions, it can be concluded that when normal people and infected people are fully mixed in a confined space, the growth rate of infected individuals is  $\beta \cdot N(t) \cdot I(t) - \gamma \cdot I(t)$ . The decline rate of normal individuals is  $\beta \cdot N(t) \cdot I(t)$ . The growth rate of recovery is  $C \cdot \gamma \cdot I(t)$ . The growth rate of death state is  $B \cdot \gamma \cdot I(t)$ . The  $B$  and  $C$  represent mortality and cure rates, and their relationship is

$$B + C = 1. \quad (8)$$

Use differential equations to express the process of normal state from infection state to recovery state and death state

$$\begin{cases} N' = \frac{dN(t)}{dt} = -\beta \cdot N(t) \cdot I(t) \\ I' = \frac{dI(t)}{dt} = \beta \cdot N(t) \cdot I(t) - \gamma \cdot I(t) \\ R' = \frac{dR(t)}{dt} = C \cdot \gamma \cdot I(t) \\ D' = \frac{dD(t)}{dt} = B \cdot \gamma \cdot I(t). \end{cases} \quad (9)$$

According to the above formula and inference, the solution of a differential equation can be solved as

$$I = (N_0 + I_0) - N + \frac{1}{\delta} \cdot \ln \frac{N}{N_0}. \quad (10)$$

In the differential (10),  $N_0$  and  $I_0$  represent the initial values, where  $\delta$  is the number of contacts at the time of infection

$$\delta = \frac{C}{\beta}. \quad (11)$$

The above is the derivation of the mathematical model formula of the improved SIR model.

In our model, social distance is not a single factor that directly affects the spread of the epidemic. Social distance in the model mainly changes the number of contacts between normal and infected people in the population, reduces the probability of being infected, and thus indirectly affects the rate of epidemic transmission. Next, the influence factor  $S_d$  (social distance) is introduced into the model, referring to the physical distance maintained between agents. As well as the number of contacts  $\delta$  during the spread of the epidemic.

In this model,  $S_d$  can be adjusted as a variable, and the range of  $S_d$  is

$$\min \leq S_d \leq \max. \quad (12)$$

In (12), min represents the minimum adjustable social distance, and max represents the maximum value. In this model, social distance directly affects the number of contacts, and their functional relationship is inversely proportional. Thus, (11) should be changed to

$$\delta = \frac{C}{\beta} \cdot (\max - S_d). \quad (13)$$

### C. COVID-19 Transmission Module

According to the above definition of agents and the modification of the SIR model, the social distance-based COVID-19 epidemic transmission model in this article has the following three transformation mechanisms, as shown in Fig. 2.

- 1) *Infection Mechanism:* That is infection state  $\xrightarrow{\text{Infect}}$  normal state. When the individual enters the scene, they are all in a normal state. At this time, none of the agents can be infected. An event was created in the population to simulate the first infected person to simulate the transmission of an epidemic. Then the infected person will send an “infection” message to the uninfected person.
- 2) *Infected Mechanism:* That is a normal state  $\xrightarrow{\text{Infected}}$  infected state. When the uninfected people receive the “infected” message, it means that a normal individual is in contact with an infected person, and it is converted into an infected person with a probability of  $\beta$ .
- 3) *Cure and Uncured Mechanisms:* That is infection state  $\xrightarrow{\text{cure}}$  rehabilitation state, infection state  $\xrightarrow{\text{notcure}}$  death state.

Some people in the infected state were cured and converted to the recovery state, while others were not cured and converted to be dead state, the period is  $W$ .

Where  $W$  (Disease cycle) refers to the transition time from the infected state to the recovery state and the dead state, the time required for the patient's physical conditions will vary. The value range is

$$n \leq W \leq m. \quad (14)$$

#### IV. EXPERIMENTS

This article uses the AnyLogic platform to create the epidemic transmission model to visualize the evolution of the epidemic. In Section IV, the social distance sensitivity analysis experiment is carried out to get the minimum social distance that should be kept. Then, the model was used to simulate the epidemic situation, and the minimum social distance was applied to the model to compare the unregulated social distance. Finally, we apply the minimum social distance to the queuing scenario and optimize the original punch card scenario.

In Section III-B, the model assumes that the simulated population is fixed and does not communicate with the outside world. Based on the effectiveness of the spread of the epidemic, we set the simulation reference at 7 days and 14 days. In Experiment IV-A, to make the obtained data more accurate, we use 21 days as the time reference point as well. Therefore, the following experiments are carried out under this premise.

##### A. Sensitivity Analysis Experiment

Sensitivity analysis is a powerful tool in investigating the impact of parameter variations on the change of system behaviors quantitatively [22]. Sensitivity analysis refers to the uncertain influence of a certain change in related factors on a certain key index or a group of key indicators from quantitative analysis. Its essence is to change the value of relevant variables one by one to solve the law of key indicators affected by these factors [23]–[25].

In the social distance-based COVID-19 epidemic transmission model, social distance impacts the number of infected people.  $I(t)$  (number of infected people) is taken as the target of sensitivity analysis, and  $S_d$  is selected as the uncertain factor.

The sensitivity analysis in this experiment is a single-factor sensitivity analysis. Other factors are fixed to determine the degree of influence of social distance on the number of infected people in uncertain factors. This experiment created a dataset of infected persons, with time as the horizontal axis and the number of infected persons as the vertical axis. The specific algorithm is as follows.

**Input.**  $S_d$ , min, max,  $L$ , DS (Dataset on the number of infected persons),  $T$ .

**Output.** Sensitivity analysis curve.

**Step 1:** Clear the previous experimental graphs and data.

**Step 2:** Read in the number of infected DS and time, draw the  $x$ -axis and  $y$ -axis of the chart.

TABLE I  
SENSITIVITY ANALYSIS DATA TABLE

Experiment	Social distance	7days	14days	21days
Run0	0.2	208	95	48
Run1	0.4	218	99	52
Run2	0.6	210	97	45
Run3	0.8	212	122	54
Run4	1.0	80	154	79
Run5	1.2	39	169	92
Run6	1.4	8	101	141
Run7	1.6	7	37	118
Run8	1.8	2	0	0
Run9	2.0	0	0	0
Run10	2.2	0	0	0

**Step 3:** Reading the  $S_d$ , min, max, step size, and calculating the number of runs required.

**Step 4:** According to the calculated  $S_d$ , draw the curve and data of the number of infected persons until  $S_d$  reaches max.

$L$  is the size of  $S_d$  the change in each experiment. In this experiment  $L = 0.2$ , min = 0.2, max = 2.2.

The value of DS is the solution set of (10)  $I$  in Section III-B,  $T$  is the number of days the model runs:  $T = 21$  days.

The sensitivity analysis in Fig. 3 has carried out a total of 11 experiments; the curve of each experiment will have corresponding data. Considering the population's size in a closed social setting, the population's mobility, and the virus's high infectivity, we set the sample size for the sensitivity analysis at 300 people. The period was 21 days. The data can be seen in Table I.

We analyzed the results of the sensitivity analysis experiment and concluded the following conclusions.

- 1) In the sensitivity analysis diagram, when the social distance does not reach its maximum, the greater the social distance, the slower the number of infections that reach their peak. The epidemic can be mitigated to some extent.
- 2) From the graph of data in Table I, when the  $S_d > 2$ , the number of infected people did not appear in the experiment. We can assume that the epidemic is under control at this social distance.

In the experiment, however, a large set of  $L$  results in a small value set of  $S_d$ , which leads to insufficient accuracy of the minimum distance. The smaller value of  $L$  is set, the minimum social distance obtained is approximately accurate.

##### B. Simulation and Comparison Experiment

In this experiment, we will verify our results by comparing the application model of minimum social distance with that without minimum social distance. The applicability of the model is also tested by setting different sample sizes.

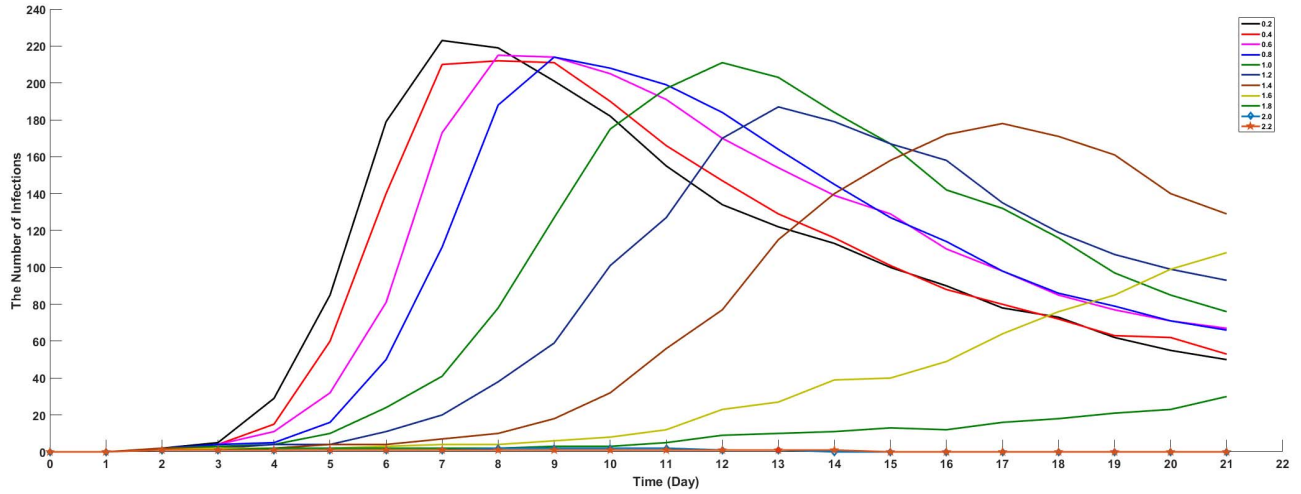


Fig. 3. Sensitivity analysis diagram.

TABLE II  
TABLE OF SIMULATION EXPERIMENT PARAMETERS

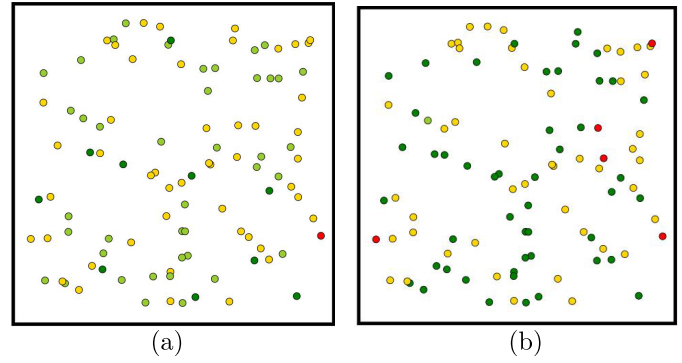
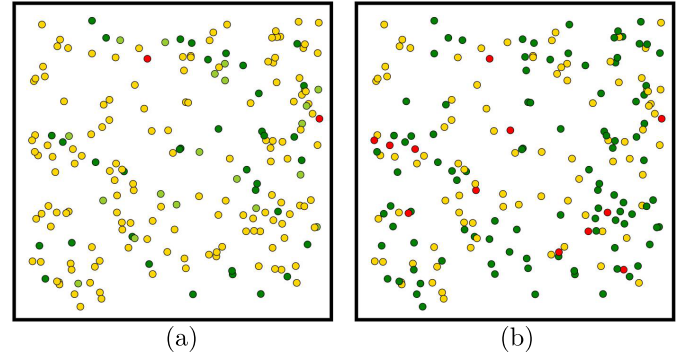
Parameter	Meaning	Value
$P(t)$	Total population	$V_{P(t)}$
$N_0$	Initial normal	$V_{P(t)} - 1$
$I_0$	Initial infected	1
$R_0$	Initial rehabilitee	0
$D_0$	Initial death	0
$\beta$	Infection rates	0.03
$W$	Disease cycle	5-12
$B$	Death rate	0.10
$C$	Cure rate	0.90
$S_d$	Social distance	$V_S$

The experiment's premise was that it was carried out without drugs, treatments, masks, etc., and the epidemic was slowed down only by adjusting the social distance.

The epidemic simulation experiment can see each important stage of the model operation. And, the setting of experimental parameters will affect the results of the model operation. In this experiment, the values of each parameter are set as shown in Table II.

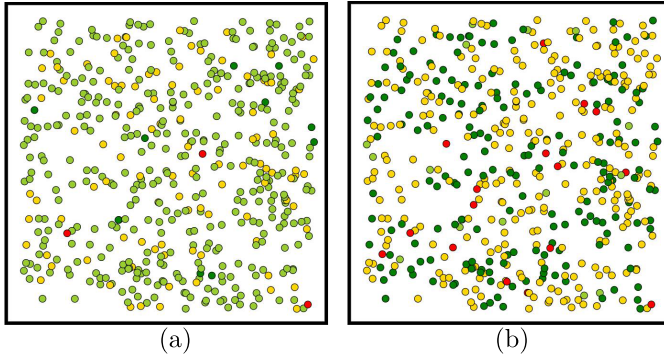
In Table II,  $V_{P(t)}$  and  $V_S$  represent the value of the total population and social distance. The value of  $V_{P(t)}$  is  $\{100, 200, 500\}$ . The value of  $V_S$  is  $\{1, 2\}$ . Besides, the value of agent parameters is set  $M[(x_1, 6), (y_1, -), (z_1, 10)]$ . The value of building parameters is set  $B\{X(20, 550), Y(40, 550), Z(0, 20)\}$ .

Due to the rapid mutation of COVID-19 (e.g., the infection rate and mortality rate of the now popular mutant COVID-19 delta is different from the original virus and worse, the virus is still mutating). We do not have access to clinical medical data from individual countries and regions. Therefore, we did not set the real virus parameters for a particular country or region.

Fig. 4.  $P(t) = 100, S_d = 1$ . (a) 7th days. (b) 14th days.Fig. 5.  $P(t) = 200, S_d = 1$ . (a) 7th days. (b) 14th days.

Instead, the experimental parameters set in this thesis were determined by calculations based on the COVID-19 statistics given by the World Health Organization. Different countries and regions use the model to develop outbreak prevention and control programs to calculate the model parameters based on clinical medical data.

The experiment first takes the parameter  $P(t)$  as a single variable and tests the applicability of the model to different people by changing the value of  $P(t)$ . After the model runs, the event is triggered and  $I_0 = 1, S_d = 1$ . The experimental results are shown in Figs. 4–6.

Fig. 6.  $P(t) = 500, S_d = 1$ . (a) 7th days. (b) 14th days.

In Figs. 4–6, light green represents normal status, yellow represents infection status, red represents death status, and dark green represents recovery status. We conducted comparative experiments on different sample agents under the condition of  $S_d = 1$ . We took the 7th and 14th days of epidemic spread as the representative. The results suggest that if social distancing is left unchecked, the epidemic will spread through the population until everyone is infected.

Besides, we also conduct quantitative verification on the number of agents in different samples from the timeline graph. In the timeline chart, we use the time axis as the horizontal axis and the total number of people as the vertical axis to draw the image with the number of people in four different states. As shown in Fig. 7.

The timeline graph in Fig. 7 shows the trend of population change in each state. It can be seen that the trend of the line graph drawn under different population conditions is roughly the same, which further verifies the applicability of the model.

Next, taking the sample of 500 people as an example, we added the minimum  $S_d = 2$  obtained in Section IV-A to the model and compared it with  $S_d = 1$ . As shown in Fig. 8.

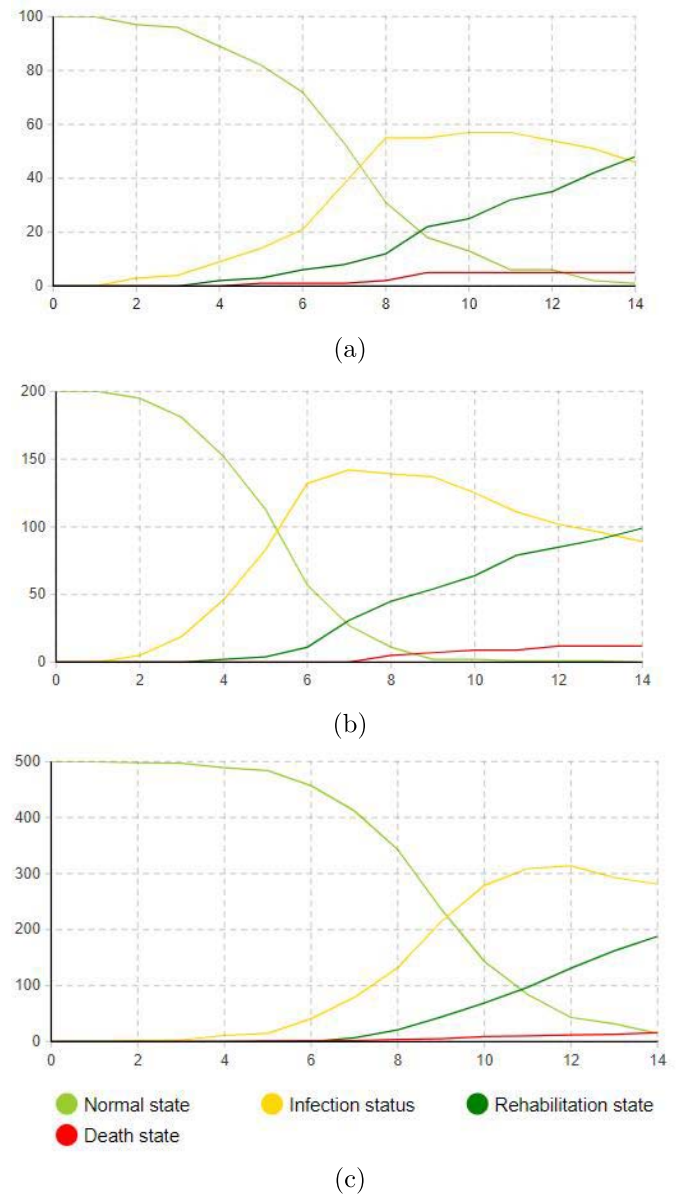
From Fig. 8 visual comparison, we found that when  $S_d = 2$  was used to adjust the epidemic model, no new infections were found on the 7th and 14th days. The experiment showed that the minimum social distance we obtained in Section IV-A was effective.

Again, we can use the Timeline graph to verify the whole process. As shown in Fig. 9(b), the number of infected people did not change when the  $S_d = 2$ .

### C. Queue Optimization Experiment

The queue optimization experiment is a scenario application of the minimum social distance. Setting the minimum social distance in the queue for punching in the factory, the matching equipment resources are adjusted and presented visually. Punch in the queue has the following characteristics: 1) there are many people, and the range of crowded activities is relatively fixed and 2) there are more contacts between people, and the contact time is longer. If there is an infected person, the chance of being infected is higher.

In this experiment, we use the results of the sensitivity analysis experiments in Section IV-A as a premise to further

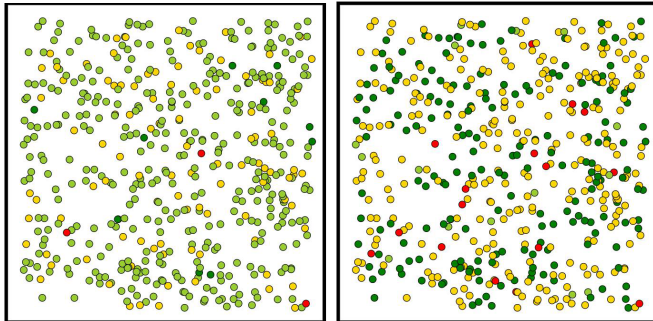
Fig. 7. Timeline graph. (a)  $P(t) = 100$ . (b)  $P(t) = 200$ . (c)  $P(t) = 500$ .

optimize the model for specific scenario applications. The queue scene optimization needs to be achieved: Let the crowd pass as quickly as possible, avoid waste of resources, and reduce crowd contact according to the minimum social distance.

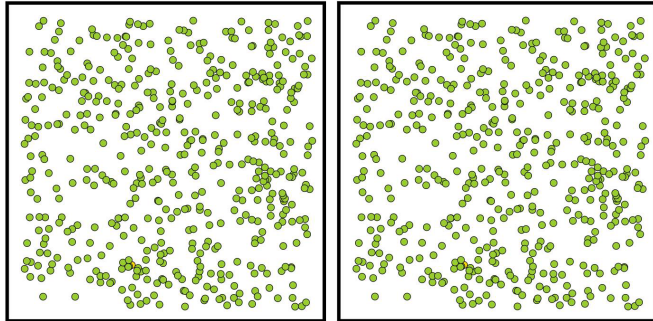
In this experiment, the queue punching scenario is selected for optimization and comparison. The business process of the queue punching scenario is as follows.

- 1) Sets the source of the agent.
- 2) Planning the travel route and destination of the agent.  
The agent arrives at the check-in queue, queues up, and enters the workshop after the check-in is completed.
- 3) Destroy the agent. When the agent completes the business process, the agent is recovered and destroyed.

The flow of the clock in the queue scenario conforms to discrete event modeling. Discrete event simulation focuses

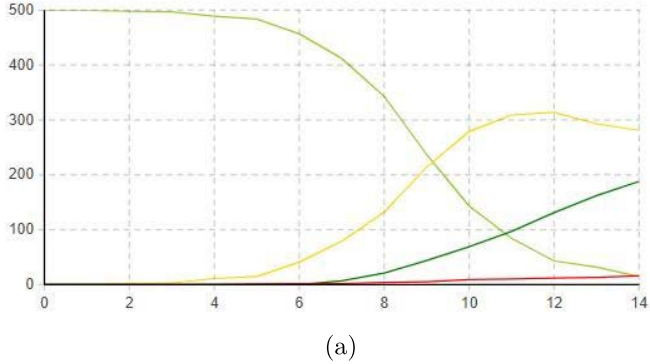


(a)

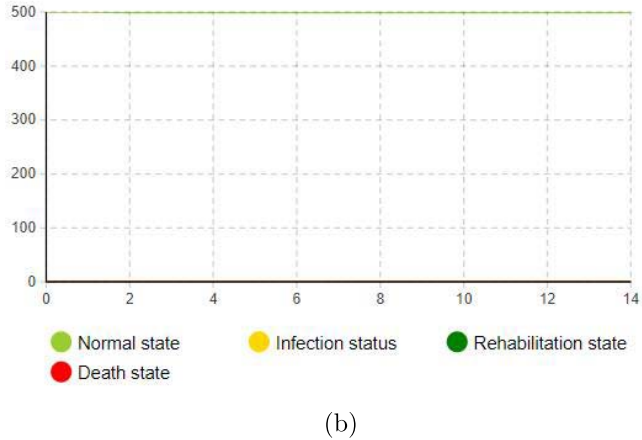


(b)

Fig. 8. Comparison experiment. (a)  $P(t) = 500, S_d = 1$ . (b)  $P(t) = 500, S_d = 2$ .



(a)



(b)

Fig. 9. Timeline comparison experimental graph. (a)  $P(t) = 500, S_d = 1$ . (b)  $P(t) = 500, S_d = 2$ .

on the abstract level of the process in the system, which usually does not represent specific physical details. As shown in Fig. 10.

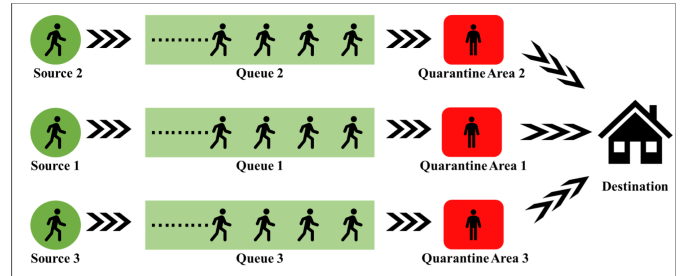


Fig. 10. Queue punching scene flowchart.

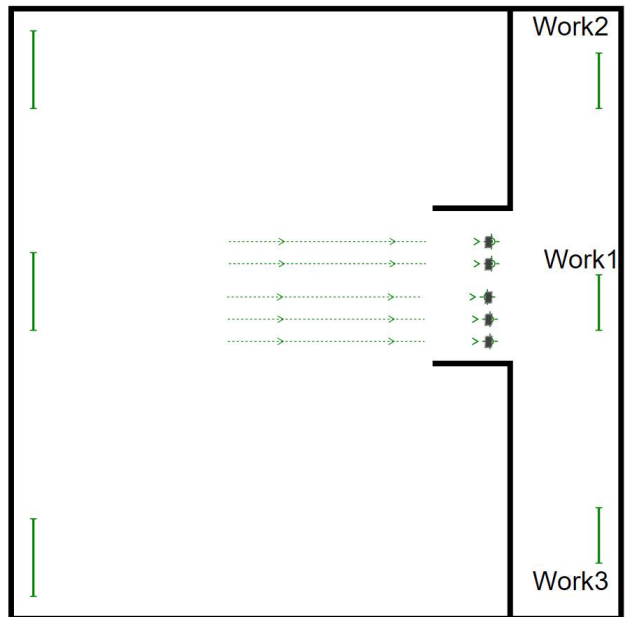


Fig. 11. Queue visualization 2-D scene.

The visualization of the queue punching scene requires visualization of the business process. According to the process and scene requirements, the scene should have an intelligence source area, queuing area, queue, security check area, detection instrument, and workshop. As shown in Fig. 11.

Queue optimization experiment has three assumptions.

- 1) Assuming that there are 500 people in the scene, the number of queues.
- 2) Assuming there is only one punching-in queue in the not optimized punching-in queue scene, the interval of the crowd in the queue is 0.2 m, the queue length is 100 m, there is no temperature detection at this time, and the passing time is 3–6 s.

After the epidemic prevention and control adjustment increase the number of queues and increase the crowd spacing, the length of queues will change. There will be epidemic prevention measures such as temperature detection, disinfection, and information registration when checking in, and the time of checking in will also change.

- 3) Assuming the interval between the crowds in the queue is 2 m. At this time, the temperature detection is set at

TABLE III  
DIFFERENT QUEUES COMPARE THE DATA TABLE

Queue number	Crowd interval(m)	Queue length(m)	Check Time(s)	Total time(s)
1	0.2	100	3-6	2596
2	2.0	500	6-9	3500
3	2.0	333.3	6-9	2333.3
4	2.0	250	6-9	1750
5	2.0	200	6-9	1400
6	2.0	166.7	6-9	1166.7
7	2.0	142.9	6-9	1000
8	2.0	125	6-9	875

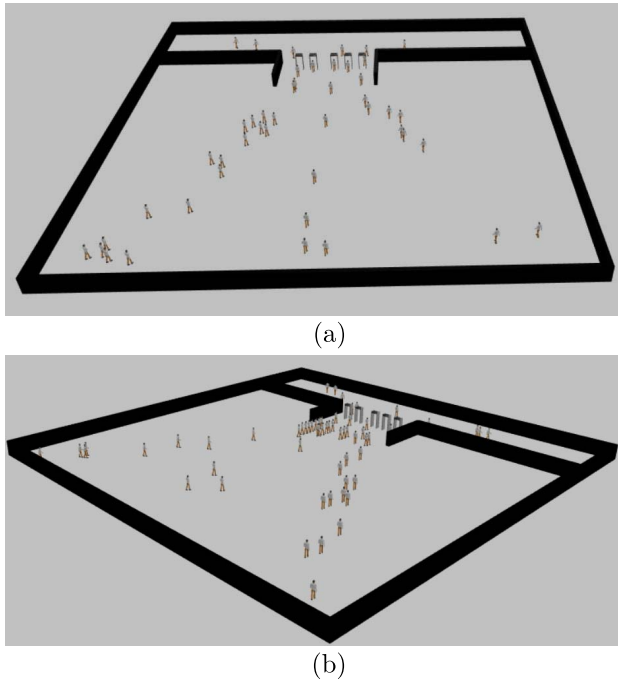


Fig. 12. Queue visualization 3-D scene. (a) Front view. (b) Right view.

the check-in, and the passing time is 6–9 s. The data can be seen in Table III.

The crowd queue simulation experiment can observe the various steps of the queue punching process. The setting of the experimental parameters will affect the simulation run results, according to the data in Table III, the queue scene simulation visualization is performed because the number of queues is 5. The experimental parameter settings are shown in Table IV.

A 3-D window was added to the experimental simulation results. Since the crowd separation was set to the minimum social distance of 2 m, there was no crowd infection in the parallel simulation scenario as shown in Fig. 12.

The newly added punching channels need to be equipped with instruments, staff, and other resources, so the number of channels is not as good as more. The setting of the number of channels needs to be selected according to the actual scene.

TABLE IV  
QUEUE VISUALIZATION EXPERIMENT PARAMETERS TABLE

Parameter	Meaning	Value
$P(t)$	Total population	500
$S_d$	The queue clearance	2
Time	Testing time	6–9
Service	Testing equipment	5
Queue	The queue numbers	5
Work	The number of workshops	3
Source1	Agent source1	200
Source2	Agent source2	100
Source3	Agent source3	200

## V. CONCLUSION

In this article, this study was conducted to determine the appropriate social distance by sensitivity analysis and apply minimal social distance to the model to suppress the transmission of the COVID-19 epidemic. The main contributions of this article are as follows: 1) we add the important factor of social distance to the modified SIR model and propose a COVID-19 epidemic transmission model based on social distance and 2) we simulated the model and obtained the minimum social distance (2 m) that should be achieved for epidemic prevention and control through sensitivity analysis. The effective social distance we provide can be applied to public health information and advice on epidemic prevention and control measures.

According to the conclusion of our model, it is safe to maintain a social distance of more than 2 m, but in densely populated and high-risk areas, we should also wear masks while maintaining a safe distance. In addition, a limitation of this study is that agents in social places may be infected by contact with the outside world. At the same time, the population set in this model is fixed and does not consider external influences. Although the current scope of the work in this article is in a small-scale scenario, the findings suggest that our model contributes to the prevention and control

of COVID-19. Further research might expand the scope of social places, such as setting the research object as the whole community to apply the research results more widely.

## REFERENCES

- [1] H. R. van Doorn, "Emerging infectious diseases," *Medicine*, vol. 42, no. 1, pp. 60–63, Jan. 2014.
- [2] S. P. Brown, "Emerging infectious diseases: Is history repeating itself?" *Lancet Infectious Diseases*, vol. 14, no. 3, p. 196, Mar. 2014.
- [3] I. Abubakar *et al.*, "Global perspectives for prevention of infectious diseases associated with mass gatherings," *Lancet Infectious Diseases*, vol. 12, no. 1, pp. 66–74, Jan. 2012.
- [4] K. B. Gibney and R. Hall, "Infectious diseases in China in the post-SARS era," *Lancet Infectious Diseases*, vol. 17, no. 7, pp. 675–676, Jul. 2017.
- [5] B. McCloskey, O. Dar, A. Zumla, and D. L. Heymann, "Emerging infectious diseases and pandemic potential: Status quo and reducing risk of global spread," *Lancet Infectious Diseases*, vol. 14, no. 10, pp. 1001–1010, Oct. 2014.
- [6] C. M. Peak *et al.*, "Individual quarantine versus active monitoring of contacts for the mitigation of COVID-19: A modelling study," *Lancet Infectious Diseases*, vol. 20, no. 9, pp. 1025–1033, Sep. 2020.
- [7] C. Sansom and D. Koech, "Kenya rises to infectious diseases challenge," *Lancet Infectious Diseases*, vol. 2, no. 9, pp. 574–575, Sep. 2002.
- [8] D. K. Chu *et al.*, "Physical distancing, face masks, and eye protection to prevent person-to-person transmission of SARS-CoV-2 and COVID-19: A systematic review and meta-analysis," *Lancet*, vol. 395, no. 10242, pp. 1973–1987, Jun. 2020.
- [9] P. Block *et al.*, "Social network-based distancing strategies to flatten the COVID-19 curve in a post-lockdown world," *Nature Hum. Behav.*, vol. 4, no. 6, pp. 588–596, Jun. 2020.
- [10] J. R. Andrews and S. Basu, "Transmission dynamics and control of cholera in Haiti: An epidemic model," *Lancet*, vol. 377, no. 9773, pp. 1248–1255, Apr. 2011.
- [11] J.-B. Wang and X. Li, "Uncovering spatial invasion on metapopulation networks with SIR epidemics," *IEEE Trans. Netw. Sci. Eng.*, vol. 6, no. 4, pp. 788–800, Oct. 2019.
- [12] Z. Chen, K. Zhu, and L. Ying, "Detecting multiple information sources in networks under the SIR model," *IEEE Trans. Netw. Sci. Eng.*, vol. 3, no. 1, pp. 17–31, Jan. 2016.
- [13] J. Xue, H. Yin, P. Lv, M. Xu, and Y. Li, "Crowd queuing simulation with an improved emotional contagion model," *Sci. China Inf. Sci.*, vol. 62, no. 4, pp. 193–195, Feb. 2019.
- [14] S. Chen, M. Small, and X. Fu, "Global stability of epidemic models with imperfect vaccination and quarantine on scale-free networks," *IEEE Trans. Netw. Sci. Eng.*, vol. 7, no. 3, pp. 1583–1596, Jul. 2020.
- [15] L. Kou, W. Fan, and S. Song, "Multi-agent-based modelling and simulation of high-speed train," *Comput. Electr. Eng.*, vol. 86, Sep. 2020, Art. no. 106744.
- [16] G. M. Nakamura, A. C. C. Souza, F. C. M. Souza, R. F. Bulcao-Neto, A. S. Martinez, and A. A. Macedo, "Using symmetry to enhance the performance of agent-based epidemic models," *IEEE/ACM Trans. Comput. Biol. Bioinf.*, early access, Aug. 24, 2020, doi: 10.1109/TCBB.2020.3018901.
- [17] J. Kwon, C. Grady, J. T. Feliciano, and S. J. Fodeh, "Defining facets of social distancing during the COVID-19 pandemic: Twitter analysis," *J. Biomed. Informat.*, vol. 111, Nov. 2020, Art. no. 103601.
- [18] J. A. Lewnard and N. C. Lo, "Scientific and ethical basis for social-distancing interventions against COVID-19," *Lancet Infectious Diseases*, vol. 20, no. 6, pp. 631–633, Jun. 2020.
- [19] Y. T. Yang and R. D. Silverman, "Social distancing and the unvaccinated," *New England J. Med.*, vol. 372, no. 16, pp. 1481–1483, Apr. 2015.
- [20] M. Salari, R. J. Milne, C. Delcea, L. Kattan, and L.-A. Cotfas, "Social distancing in airplane seat assignments," *J. Air Transp. Manage.*, vol. 89, Oct. 2020, Art. no. 101915.
- [21] S. K. Chandra, A. Singh, and M. K. Bajpai, "Mathematical model with social distancing parameter for early estimation of COVID-19 spread," in *Machine Vision and Augmented Intelligence—Theory and Applications*. Singapore: Springer, Nov. 2021, pp. 23–31.
- [22] B.-Y. Lu and H. Yue, "Developing objective sensitivity analysis of periodic systems: Case studies of biological oscillators," *Acta Automat. Sinica*, vol. 38, no. 7, p. 1065, 2012.
- [23] V. Cavaliere, M. Cioffi, A. Formisano, and R. Martone, "Improvement of MRI magnet design through sensitivity analysis," *IEEE Trans. Appl. Supercond.*, vol. 12, no. 1, pp. 1413–1416, Mar. 2002.
- [24] S. Avila *et al.*, "Sensitivity analysis applied to decision making in multiobjective evolutionary optimization," *IEEE Trans. Magn.*, vol. 42, no. 4, pp. 1103–1106, Apr. 2006.
- [25] Z. Liu and F. Tu, "Single sample path-based sensitivity analysis of Markov processes using uniformization," *IEEE Trans. Autom. Control*, vol. 44, no. 4, pp. 872–875, Apr. 1999.



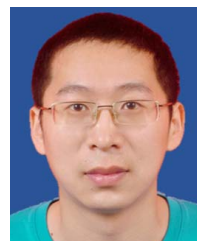
**Junxiao Xue** (Member, IEEE) received the Ph.D. degree in computational mathematics from the School of Mathematical Sciences, Dalian University of Technology, Dalian, China, in 2009.

He is currently an Associate Professor with the School of Cyberspace Security, Zhengzhou University, Zhengzhou, China. He has authored more than 40 journal and conference articles in these areas, including the IEEE TRANSACTIONS ON KNOWLEDGE AND DATA ENGINEERING (TKDE), the IEEE TRANSACTIONS ON COMPUTATIONAL SOCIAL SYSTEMS (TCSS), *Science China-Information Sciences* (SCIS), *Frontiers of Information Technology and Electronic Engineering* (FITEE), etc. His current research interests include computer graphics, virtual reality, and social network analysis.



**Mingchuang Zhang** is currently pursuing the master's degree with the School of Cyberspace Security, Zhengzhou University, Zhengzhou, China.

His research interests include simulation modeling, swarm intelligence, and multiagent reinforcement learning.



**Mingliang Xu** (Member, IEEE) received the Ph.D. degree in computer science and technology from the State Key Laboratory of CAD & CG, Zhejiang University, Hangzhou, China, in 2012.

He is currently a Vice President and a Professor with the School of Information Engineering, Zhengzhou University, China, and the Vice General Secretary of ACM SIGAI China. He has authored more than 60 journal and conference articles in these areas, including ACM *Transactions on Graphics* (TOG), ACM *Transactions on Intelligent Systems and Technology* (TIST), the IEEE TRANSACTIONS ON PATTERN ANALYSIS AND MACHINE INTELLIGENCE (TPAMI), the IEEE TRANSACTIONS ON IMAGE PROCESSING (TIP), IEEE TRANSACTIONS ON CYBERNETICS (TCYB), IEEE TRANSACTIONS ON CIRCUITS AND SYSTEMS FOR VIDEO TECHNOLOGY (TCSVT), ACM SIGGRAPH (Asia), the ACM International Conference on Multimedia (MM), the IEEE International Conference on Computer Vision (ICCV), etc. His current research interests include computer graphics, multimedia, and artificial intelligence.